Journal of Materials Chemistry B

Accepted Manuscript

ROYAL SOCIETY OF CHEMISTRY

www.rsc.org/materialsB

rnal of Materials Chemistry B RSCPublishing

ARTICLE

A high efficiency approach for titanium surface antifouling modification: PEG-*o*-quinone linked with titanium via electron transfer process

Songtao Liu, Lijuan Chen, Lin Tan, Fuhu Cao, Longchao Bai, Yanmei Wang*

Cite this: DOI: 10.1039/xoxxoooooox

Received ooth January 2012,
Accepted ooth January 2012

DOI: 10.1039/xoxxoooooox

www.rsc.org/

We explored a novel approach for modification of titanium surfaces to improve the biocompatibility and antifouling properties by using the PEG-catechol. As all know, PEG-catechol can self-assemble onto titanium surfaces easily. However, the higher grafting density by this approach is hard to be obtained. In our paper, *o*-quinone (the oxide of catechol) as adhesive segment was the first time used to graft PEG brushes onto titanium surfaces using electroreduction process. Variable angle spectroscopic ellipsometer showed that the ultrahigh-density PEG brush adlayer could be grafted to the titanium surface when the *o*-quinone segment performed electrochemical reduction on the titanium. We called the adlayers that grafted onto titanium surfaces by this kind of approach electro-assembly monolayers (e-AMs). This is in order to distinguish with the PEG-catechol self-assembly monolayers (SAMs). The XPS, AFM and WCA techniques were also used to characterize the coating grafted onto the titanium surfaces via the two different ways. A clear result is that the grafted density of e-AMs can be reached highly than that of SAMs, and the grafted density of e-AMs can be easily modulated. In addition, the long-term stability of e-AMs against full blood serum, FITC marked BSA and platelet adsorption was better than that of SAMs.

Introduction

Titanium (Ti) and Ti alloy materials are types of biomaterials that have been developed for surgical implants and dental applications.[1-3] However, nonspecific adsorption of proteins on Ti based biomaterials surface limited the long-term applications of Ti based biomaterials surface. To prevent non-specific protein absorption and to confer excellent biocompatibility to the Ti-based medical devices, bioinert thin polymer coatings are becoming more and more popular. As reported, polymer coatings can generate excellent surface properties, such as corrosion protection, biocompatibility,[4] non-biofouling,[5, 6] recognition, selective bacterial adhesion,[7, 8] reversible switch,[9, 10] and chromatography supports.[11] Thus, numerous approaches have been developed to modify the titanium surfaces with polymers. Among them, the different interactions between polymers and titanium surfaces are often used to modify the titanium surfaces. For example, electrostatic forces and hydrogen-bond can be used to form layer by layer polymer coating on substrate surfaces,[12, 13] silane coupling agents can be used to bind polymer coating on substrate surfaces through covalent bonds,[14] and so on. Recently, catechols have been found applications for the modification of titanium substrates,[15-19] because catechol can chelate with TiO_2 (The titanium and Ti alloy surfaces always covered by a thin layer of TiO_2).

Catechol (including dopamine and its derivatives), an important functional component of mussel-adhesive proteins, have been found to have many applications in the surface modification field due to its outstanding adhesion performance.[17] For example, dopamine can react with atom transfer radical polymerization (ATRP) or a reversible addition fragmentation chain transfer polymerization (RAFT) initiator to form a mimetic initiator, which can self-assemble on the titanium substrate surfaces to form a stable initiator layer and then undergo further surface-initiated polymerization (SIP) to confer different properties to the surface.[20, 21] Dopamine can directly polymerize on a wide variety of material surfaces to form a type of adhesive functional polydopamine (PDA) coating, which can be used as a chemical active foundation layers for secondary surface-mediated reactions.[22-28] Dopamine can combine with a polymer chain to form mussel adhesive protein mimetic polymers (polymer-catechol), which have been developed as a self-assembly strategy for the formation of a polymer brush coating on titanium surfaces by the chelating interaction between catechol and titanium cation.[5, 29] The third strategy from above is deemed a promising approach to modifying TiO_2 surfaces, due to its simple one-step operation. Poly(ethylene glycol) (PEG) functionalized catechol is frequently used for the production of non-fouling TiO_2 surfaces via the self-assembly strategy, in view of PEG's outstanding properties including neutrality and solubility in water, low toxicity, and immunogenicity.[13, 30] However, the low grafting density and instability of the linear PEG-catechol self-assembly limit its application.

Recently,[18] ethylene glycol dendron-(catechol)$_x$ conjugates on TiO_2 surfaces demonstrated the importance of the multivalent oligocatechol binding and the ethylene glycol dendron-type compounds for both stable adsorption and excellent antifouling properties. By reason that multiple catechol segments increased the probability of chelate reaction between catechol and metal cation of surfaces; and the complex molecular architectures of PEG is good for improving surface coverage. Nevertheless, it is cumbersome to synthesize ethylene glycol dendron-(catechol)$_x$ compounds. Therefore, it would be a significant development if a simple polymer, such as linear PEG-catechol could modify TiO_2 surfaces with a high brush density via a simple and high-efficiency approach.

As reported, ortho-benzoquinone (*o*-quinone, the oxide of catechol) can react with some active metals to form catechol chelate compounds due to the electron transfer between *o*-quinone and the metal. For example, tetrahalogeno-ortho-*o*-quinone can accept electrons from metallic tin and indium to form the corresponding tin (Ⅳ) or indium (Ⅲ) catechol chelate complexes, similar to the direct formation of the catechol chelate with tin (Ⅳ) or indium (Ⅲ).[31] Inspired by the aforementioned concepts, PEG-*o*-quinone electroreduction on the titanium electrode surface has been studied in our paper, because we hope the quinone segment can obtain electron from the titanium cation of the surfaces to form catechol-titanium chelate compounds in high reaction efficiency. In addition, as we know,[32, 33] electrochemical reaction is a powerful method that can improve the efficiency of the electrode reaction and has been widely used for surface modification of electrodes, since the redox reaction can be controlled easily on the electrode surfaces. As mentioned before, the efficiency of catechol self-assembly onto the surfaces is not high, which results in a difficulty for PEG-catechol formed a dense single monolayer on substrates. Thus, it draws our attention to improve the efficiency of the chelate reaction of PEG grafting on titanium substrates via an electron transfer process.

In this work, PEG-*o*-quinone was used to graft PEG brushes onto the titanium substrates through electroreduction. In the meantime, two kinds of PEG-DOPAquinone (one with an amine, one with a carboxyl) were prepared to investigate the influence of different group of the quinone. The monolayers formed by this approach are electro-assembly monolayers (e-AMs for short). Consequently, we found it is a high-efficiency strategy for PEG brushes modification titanium surfaces via PEG-*o*-quinone electrochemical reduction on the surfaces, which can graft higher density PEG brush than PEG-catechol self-assemble onto titanium surfaces. Furthermore, the e-AMs of PEG-*o*-quinone possess the excellent full blood serum and FITC marked BSA and platelet adsorption resistant properties, and at the same time the resistant properties of e-AMs can keep a long-term stability, which is very important for the applications of Ti-based medical devices in a long time.

Materials and methods

Materials

PEG-DOPA (COOH) (P1) and PEG-DOPA (NH_2) (P2), PEG-DA (P3) ($\overline{M}_w$ of PEG chain is ~2000) were synthesized according to previously published procedure.[34, 35] The preparation and characterization of the PEG-catechols are presented in the Electronic Supplementary Information (ESI, Fig. S1). PEG-DOPAquinone (COOH) (P1'), PEG-DOPAquinone (NH_2) (P2'), PEG-*o*-quinone (P3') solution were obtained from the oxidation of PEG-catechols solution (Scheme 1), as described in the ESI (Fig. S2 and Fig. S3). *N*-(2-hydroxyethyl)-piperazine-*N'*-(2-ethanesulfonic acid) (HEPES, ≥99.5%) were purchased from Sigma-Aldrich (St. Louis, MO, USA). Morpholine ethanesulfonic acid monohydrate (MES, 99%) was purchased from Vetec (Shanghai, China). Titanium (Ti) substrates were produced by magnetron sputtering, the details were shown in the ESI (Fig. S4). Gold substrates were produced by glass slides coated with an adhesion-promoting chromium layer (thickness 5 nm) and a gold (Au) layer (45 nm) by electron beam evaporation. A full blood serum (from a healthy human) solution was prepared freshly using Millipore water and was filtered prior use. Fluorescein isothiocyanate-labeled bovine serum albumin (FITC-BSA) was prepared according to previously published procedures.[36] Platelet-rich plasma obtained from the fresh human blood by centrifugation at 800 rpm for 10 min. All of the water used was triple pure water.

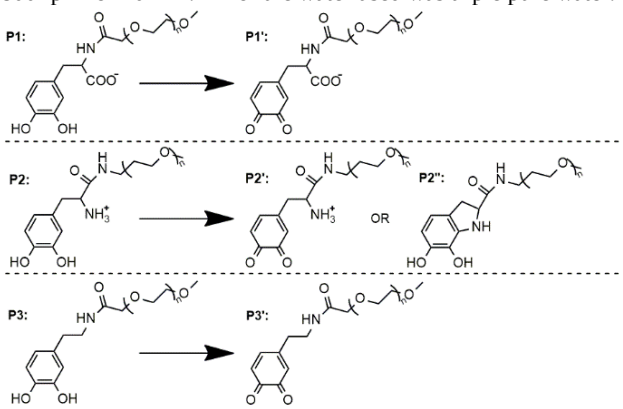

Scheme 1. The molecular structure of different PEG-catechols and PEG-*o*-quinone.

The CVs of the PEG-*o*-quinone solution

A CHI600D electrochemical workstation (Chenhua, Shanghai, China) was used to measure the cyclic voltammetry (CV) scans of three types of PEG-*o*-quinone (P1', P2', and P3') solutions at 60 ℃. Pt and KCl-saturated Ag/AgCl electrodes were used as the counter and reference electrodes, respectively. A Ti substrate was used as the work electrode. Aliquots of 2 mmol/L P1', P2', and P3' MES buffer solutions (50 mmol/L MES, pH 6.0) were used as the electrolyte. The potential window was -1.2 to 1.2 V (vs. Ag/AgCl), and the scanning rate was 100 mV/s. An illustration of the CV scanning devices is shown in the ESI (Fig. S5).

The preparation of modified substrates

2 mmol/L P1', P2', and P3' MES buffer solutions (50 mmol/L MES, pH 6.0) were used to perform electro-assembly onto substrates (including Ti and Au) using electrochemical potentiostatic technology. Pt and KCl-saturated Ag/AgCl electrodes were used as the counter and reference electrodes, respectively. A Ti (or Au) substrate was used as the work electrode. P1', P2', and P3' MES buffer solutions (pH 6.0) were used as the electrolyte, respectively. The modification of P1', P2', and P3' onto the substrates was performed for different time at 60 ℃. Then the e-AMs modified substrates were produced. As for the preparation of self-assembly monolayers (SAMs) modified substrates, the operation was performed according to the previous reference,[19] and 2 mmol/L P1, P2, and P3 MES buffer solutions were used respectively. The substrates were immersed in the solution at 60 ℃ under nitrogen atmosphere to produce SAMs modified substrates. After modification, the substrates were incubated in pH 6.0 MES buffer solution for 40 min, subsequently rinsed with triple pure water, and dried under a stream of nitrogen.

Variable angle spectroscopic ellipsometer

The adlayers thicknesses of modified substrates (including the e-AMs and SAMs modified Ti and Au substrates) were determined using a variable angle spectroscopic ellipsometer (M-2000, Woollam Co., Inc., Lincoln, NE). The measurements were performed in the spectral range of 370 to 1000 nm at two different angles of incidence (70 °and 80 °). The analysis software Complete EASE 4.81 was used to analyse all of the data to determine the thickness (*a*) of the adlayers. Each data point was the average of the measurements of at least three different samples, and each sample was measured at least nine times. The statistical evaluation was performed by one-way ANOVA comparison of the sample data. The brush grafting density (*n*) was expressed concretely as follows: [18]

$$n = \frac{a\rho N_A}{\overline{M}_w} \qquad (1)$$

where *a* is the thickness of a dried PEG adlayer, ρ is the assumed density of the dried PEG adlayer (1.08 g/cm^3),[18] N_A is Avogadro's constant, and $\overline{M}_w$ is the weight-averaged molecular weight of PEG-*o*-quinone.

The optical constants of the sputtered Ti (Au) substrates were fitted using a B-Spline model.[37] The fitted optical constants were saved as the Ti (Au) substrates model. The TiO_2 adlayers was fitted to obtain the thickness value of TiO_2 by oscillator model, and the organics adlayer (including polymer adlayers and serum adsorption adlayers) was fitted using the Cauchy model (A = 1.45, B = 0.01, and C = 0).[18, 38, 39] Each sample was measured at least nine times.

Water contact angle for surfaces

Water contact angle (WCA) measurements formed by a water droplet (2 μL) on the surfaces were measured using a SL200ks goniometer from KINO (U.S.A). Each data point was the average of the measurements of at least three different samples, and each sample was measured at least six times.

Atomic force microscope

The surface morphology and the roughness of the modified Ti substrates were studied using an atomic force microscope (AFM) in tapping mode (DI Multimode V, Veeco, U.S.A.).

X-Ray photoelectron spectrometer (XPS)

The elemental composition of the Ti substrates was determined using a VG ESCALAB MK II XPS (VG Scientific Instruments, England) with an Al (Kα) X-ray source (1486.6 eV). All spectra were calibrated by setting the signal of the aliphatic C signal at 284.7 eV (rather than 285.0 eV, given the high proportion of aromatic carbon in the compounds).

Stability of the PEG adlayers

The modified Ti substrates with e-AMs and SAMs were incubated in phosphate buffer solution (PBS, 0.01 M, pH 7.4) for a period of time at room temperature, and the substrates were then rinsed with triple pure water and dried under a stream of nitrogen. Subsequently, ellipsometry was used to analyse the thickness of the modified Ti substrates.

Antifouling study

Firstly, full blood serum was used. The modified Ti substrates with e-AMs and SAMs were respectively immersed in PBS (0.01 M, pH 7.4) for 15 min and subsequently incubated in 250 μL of full blood serum. After a 20 min incubation time, HEPES 2 buffer (0.1 mol/L HEPES, pH = 7.4, 150 mmol/L NaCl, H_2O) was added into above described solution, and each sample was transferred to a clean well containing HEPES 2 solution and further incubated for 20 min; and then the substrates were rinsed with water, dried under a stream of nitrogen, and subsequently analysed by ellipsometry.

Secondly, laser scanning confocal microscope (LSCM, LSM510 from Zeiss, Germany) image of the attachment tests of FITC-BSA was also used to test the anti-fouling properties of the modified substrates. The modified Ti substrates with e-AMs and SAMs were immersed respectively in PBS (0.01 M, pH 7.4) for 2 h, subsequently incubated in 0.25 mg/ mL FITC-BSA PBS solution for 2 h; and then, the substrates were rinsed with water, dried under a stream of nitrogen, and subsequently analysed by LSCM.

Thirdly, scanning electron microscope (SEM) image of the attachment tests of platelet was used to test the antifouling properties and biocompatibility of the modified substrates. The platelet-rich plasma obtained from the fresh human blood by centrifugation at 800 rpm for 10 min. The platelet adhesion samples were prepared according to the work of Ding et al[40]. The specimens were coated with gold and the morphology was observed by a scanning electron microscope (SEM) (JSM-6700F, JEOL Co., Japan).

Results and discussion

Preparation of e-AMs modified Ti substrates

Fig. 1 shows the cyclic voltammetry curves (CVs) of the MES buffer (a) and the PEG-*o*-quinone (P1' (b), P2' (c) and P3' (d)) solutions. As depicted in this figure, reduction peaks of *o*-quinone segment were observed individually in the CVs of P1', P2' and P3' (see the inset graph of Fig. 1; the reduction peaks are enlarged). It is worth noting that, the beginning potential of water electrolysis was -0.3 V (curve a, vs. Ag/AgCl) and the beginning potential of *o*-quinone reduction was 0.155 V (curve b, c, d). Among these, the peak potentials of P1', P2' and P3' were at -0.10 V, -0.25 V, and -0.15 V, respectively. The peaks current absolute value of P1' and P2' were lower than that of P3', implying that P3' has the highest electroreduction efficiency on the titanium electrode.[41] The differences of the reduction peaks could be ascribed to the different group existed in the PEG-*o*-quinone (–COO^- existed in P1', –NH_3^+ existed in P2', and there are not –COO^- or –NH_3^+ in P3'). Because different group will result in different electrostatic force and steric effect between PEG-*o*-quinone and Ti substrates, then lead to the different diffusion rate of *o*-quinone segment to the Ti substrates (ESI, Fig. S6 and S7). Compare with P1' and P2', *o*-quinone segment of P3' was easier to diffuse onto the electrode surface and carry on the reduction reaction (the reaction is controlled by diffusion rate, ESI, Fig. S8).

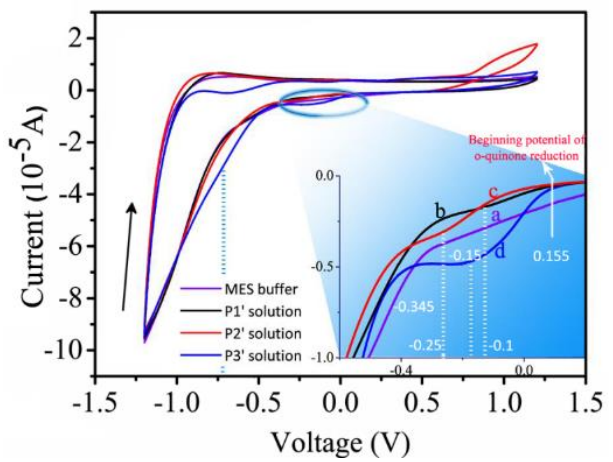

Fig. 1 The CVs of MES buffer (a) and PEG-*o*-quinone (b-P1', c-P2', d-P3') solutions (2 mmol/L in MES buffer). Inset: partial enlarged graph of the reduction peak.

In this paper, we hope *o*-quinone segment can perform the electrochemical reaction on the electrode surface with a high rate and without side reaction, therefore, the electrolysis potential range of PEG-*o*-quinone should be chosen between 0.155 V and -0.3 V. Moreover, in consideration of the different diffusion of *o*-quinone segments, the peaks potential should be used as the electrolysis potential. Thus, potentials of -0.1 V, -0.25 V, -0.15 V were used as the electrolysis potentials of the potentiostatic electro-assembly of P1', P2', and P3' in different time. The current vs time (I-t) curves of electrolysis of PEG-*o*-quinone were showed in ESI (Fig. S9).

The characterization of modified surface

The eletro-assembly adlayers (e-AMs) thickness of P1', P2', P3' of modified Ti (or Au) substrates during 20 h were measured by ellipsometry and depicted in Fig. 2. Moreover, the self-assembly adlayers (SAMs) thickness of P1, P2, and P3 of modified Ti (or Au) substrates during 20 h were also showed in the Fig.2. A very important finding was that the thickness of P3' e-AMs modified Ti substrates reached 62.1 Å which was thrice thicker than the SAMs of P3 (20.5 Å). Moreover, the e-AMs of P1' (33.7 Å) and P2' (24.2 Å) are all thicker than the SAMs of P1 (13.9 Å) and P2 (15.1 Å). Evidently, the PEG can adsorb on titanium surfaces by self-assembly and electro-assembly, and the e-AMs were thicker than the SAMs. The SAMs could graft onto the titanium surfaces because the catechol segment of P1, P2, and P3 can chelate with the titanium oxide of titanium surfaces with low polymer density. However, during the formation of e-AMs, PEG-*o*-quinone could obtain electron from Ti substrates and generate a transient state with the oxygen lone-pair electrons, which can chelate with titanium oxide in a high reaction rate and result in catechol-titanium-oxide chelate structure (Scheme 2). Therefore, the e-AMs can reach a high density and thickness. However, the graft thicknesses of P1' and P2' were lower than that of P3', it suggested that P3' could diffuse easily onto the electrode surface and perform the electroreduction, as we discussed before. The e-AMs of P3' on the Au electrode surface only with a 8.3 Å thicknesses, although *o*-quinone can obtain electron from Au electrode easier than from Ti electrode (ESI, Fig. S10). This probably attribute to the catechol cannot chelate with Au surface, and the little absorption adlayer on Au substrate is attribute to Van der Waals force and hydrogen bond interaction.[17] In a word, the e-AMs of PEG-*o*-quinone can be used to produce thicker PEG adlayer on TiO_2 surface than self-assembly of PEG-catechol, the

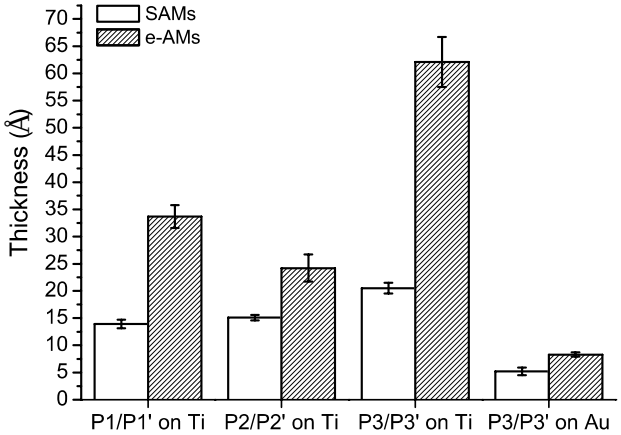

Fig. 2 The adlayer thickness of PEG modified Ti and Au substrates through SAMs (P1, P2, P3) and e-AMs (P1', P2', P3') during 20 h. ($p < 0.01$).

electrochemical reduction of *o*-quinone segment and the catechol chelate with TiO_2 showed a synergistic effect in this strategy.

XPS was used to determine the chemical composition of the modified and unmodified Ti substrates. C1s, O1s, N1s, and Ti2p XPS spectra were obtained and evaluated quantitatively. The representative XPS spectra of Ti2p (464.2 eV and 458.5 eV), O1s (529.9 eV), C1s (284.6 eV), N1s (401.6 eV) were obtained for all of the Ti substrates. The weak C1s and N1s signals in unmodified Ti substrate are due to some adventitious contamination.[18] After the PEG modification of the Ti substrate using e-AMs, significant changes in the O1s, C1s, and N1s signals were observed. The C1s signals were fitted by three components on the basis of their respective binding energies: carbon next to aromatic and aliphatic carbon (C_A, 284.6 eV), carbon of C-N or C-O bonds (C_B, 286.2 eV), and the carbonyl carbon (C_C, 288.1eV). The O1s signals were also fitted by three components: the oxygen of the TiO_2 (O_A, 529.9 eV), the carbonyl oxygen (O_B, 531.1 eV), and the oxygen of the C-O bond (O_C, 532.6 eV). The N1s signal consisted of two types of nitrogen: one was the amide nitrogen (N_A, 400.1 eV), and the other was from nitrogen contamination (N_B, 401.6 eV).[42] The fitted XPS spectra are shown in the ESI (Fig. S11). Table 1 presents the C_{total}/Ti, O_A/Ti and C_B/O_C atomic ratios of the modified and unmodified Ti substrates. Evidently, compared with that of the unmodified substrate, the C_{total}/Ti ratio of the modified Ti substrates increased. The C_{total}/Ti ratio of the P3' e-AMs substrate modified for 20 h was the highest, which means the quantity of the PEG grafted on the Ti substrates was the highest among the substrates studied. These results were consistent with the results of ellipsometry characterization. The O_A/Ti ratio was found to be close to the

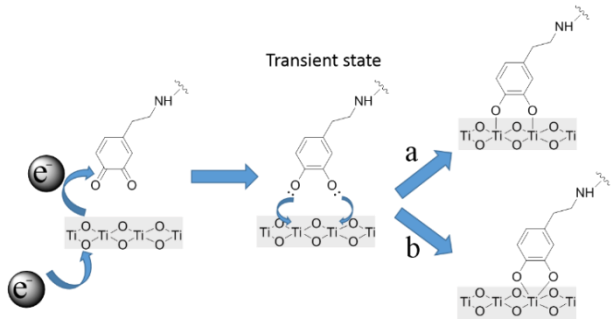

Scheme 2. The mechanism of PEG-o-quinone grafted onto titanium oxide surfaces of titanium substrates (PEG-o-quinone as the example) in a high efficiency through electroreduction and the electron transfer process.

theoretical value of 2.0 for all of the Ti substrates, while the C_B/O_C ratio was also close to the theoretical value of the C/O ratio of PEG (approximately 2.0). Therefore, the XPS results verified that PEG-*o*-quinone e-AMs have grafted more PEG brushes on the substrate.

Table 1. Atomic ratios of C_{total}/Ti, O_A/Ti, and C_B/O_C, grafted PEG brush density (n / nm^2) and water contact angle (WCA (˚)) of blank or 20 h modified Ti and Au substrates.

	C_{total}/Ti	O_A/Ti	C_B/O_C	n/nm^{2c}	WCA(˚)
Blank Ti	0.64	2.03	4.2	/	65.7±5.4
Ti (P1')[a]	4.63	2.09	2.11	1.03±0.06	27.7±3.7
Ti (P2')[a]	3.37	2.15	2.03	0.74±0.08	31.8±5.8
Ti (P3')[a]	10.04	2.22	2.36	1.9±0.14	40.9±1.2
Ti (P3)[b]	2.54	1.93	1.9	0.63±0.03	28.3±0.6
Clean Au	/	/	/	/	74.2±1.7
Au (P3')[a]	/	/	/	/	56.5±3.4

[a)] e-AMs modified substrates; [b)] SAMs modified substrates; [c)] obtained from equation (1)

The electro-assembly of PEG-*o*-quinone process was verified by their atomic force microscopy (AFM). Fig. 3A shows the AFM image of the Ti substrate without modification; Fig. 3B shows the morphology of the 2 h e-AMs modified surface of P3', and Fig. 3C shows the morphology of the 6 h e-AMs modified surface of P3', and Fig. 3D shows the morphology of the 20 h e-AMs modified surface of P3'. The results showed that the Ti nutty structures (Fig. 3A) were covered by the PEG slowly (Fig. 3B) and finally disappeared (Fig. 3C, D), the PEG formed a homogeneous film on the surface after 6 h electro-assembly. As shown in Fig. 3, the root mean square (RMS) value of the surface roughness increased from 0.747 nm (Fig. 3A) to 0.765 nm for the 2 h modification (Fig. 3B), and then decreased to 0.422 and 0.337 nm for 6 h and 20 h modification (Fig. 3C and 3D), individually. These results suggested that in the initial 2 h modification of the Ti substrate, there are not enough grafted molecules to form a full coating to cover the substrate. After the 2 h modified substrate was dried, the PEG molecules will entangle together due to intermolecular forces, and then form many protuberances on the substrate. The average height of these protuberances was higher than that of blank Ti substrate, resulting in the increment of RMS value from 0.747 nm to 0.765 nm for the 2 h modification. Furthermore, the AFM height map of Fig. 3B (ESI, Fig. S12) showed the grafted polymer was in the depression of the substrate surface, which indicates the PEG might graft into the depression of the substrate surface preferentially, where the *o*-quinine segment can obtain electron faster. RMS value then decreased with the e-AMs modification time (Fig. 3C for 6 h and Fig.3D for 20 h), and the PEG brush of 6 h e-AMs covered the substrate fully and the PEG brush was not tightness like that of 20 h e-AMs. By contrast, the surface modified by P3 self-assembly for 20 h (Fig. 3E) was slightly covered by a PEG adlayer, with an RMS value of the surface roughness of 0.653 nm. Obviously, the coverage of PEG-*o*-quinone e-AMs on the Ti substrate was higher than that of PEG-catechol SAMs for the same modification time. The distribution curves of the peak depths of the morphology (Fig. 3F) showed the depths decreased with the increment of modification time, implying that the PEG eventually covered the Ti substrate almost entirely.

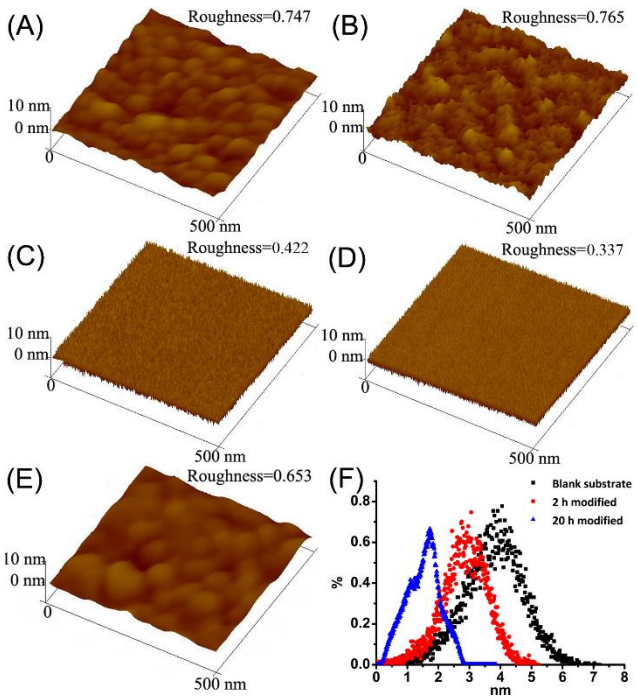

Fig. 3 (A) AFM image of a blank Ti substrate. (B) AFM image of 2 h P3' e-AMs on a Ti substrate surface. (C) AFM image of 6 h P3' e-AMs on a Ti substrate surface. (D) AFM image of 20 h P3' e-AMs on a Ti substrate surface. (E) AFM image of 20 h P3 SAMs on a Ti substrate surface. (F) The distribution curves of the peak depths of the morphology of A, B, and D.

The wetting ability of PEG adlayers

As reported, the wetting ability of PEG adlayers is very important for antifouling coating, and the WCA should decrease with the increment of PEG adlayer thickness on Ti substrates. However, the ultra-high thickness of e-AMs of P3' did not bring about a lower WCA (Table 1). This is probable that ultrahigh dense PEG brush (1.9 /nm^2) reduced the wetting ability of PEG adlayers.[43] Ultrahigh dense PEG brush probably will strengthen the intermolecular and intramolecular effect of PEG chains,[44] subsequently lead to the reduction of the hydrogen-bonding availability between PEG chains and water, therefore, hydration ability of PEG chains will be decreased, and the wetting ability of ultrahigh dense PEG will be reduced. Therefore, a more suitable PEG brush density for the preparation of the coating with excellent hydrophilicity should be explored. Thus, the adsorption kinetics of PEG adlayers modified Ti substrates by e-AMs (a: P1', b: P2', and c: P3') and SAMs (d: P3 and e: P3') during different modification time were studied and shown in Fig. 4A. It can be observed that the adsorption rate of e-AMs (Fig. 4A a-c) was higher than that of SAMs (Fig. 4A d and e) and P3' cannot self-assemble onto Ti substrate (Fig. 4A e). Meanwhile, the WCA of P3' modified surfaces using e-AMs during different time were also shown in Fig. 4B. As shown in Fig. 4B, the WCA of P3' e-AMs modified surfaces decreased with the increment of PEG adlayer thickness at the first 6 h. However, the WCA increased when the incubation time longer than 10 h. The lowest average WCA value was 22.2˚ with 28.4 Å e-AMs thickness and 0.87 / nm^2 PEG brush density for 6 h modified time, which cannot be obtained by self-assembly of P1, P2, and P3. Obviously, a suitable PEG adlayer thickness or brush density is necessary for obtaining a surface with an excellent wetting ability. The variation of surfaces topography of the modified surfaces with the modification time (Fig.3) can also illustrate the change of wetting ability. As shown in Fig. 3B, the titanium surface was not covered totally by PEG for the first 2 h, thus the wettability of 2 h modified surfaces was not good enough (Fig. 4B). The surface was covered almost with the PEG chains (Fig.

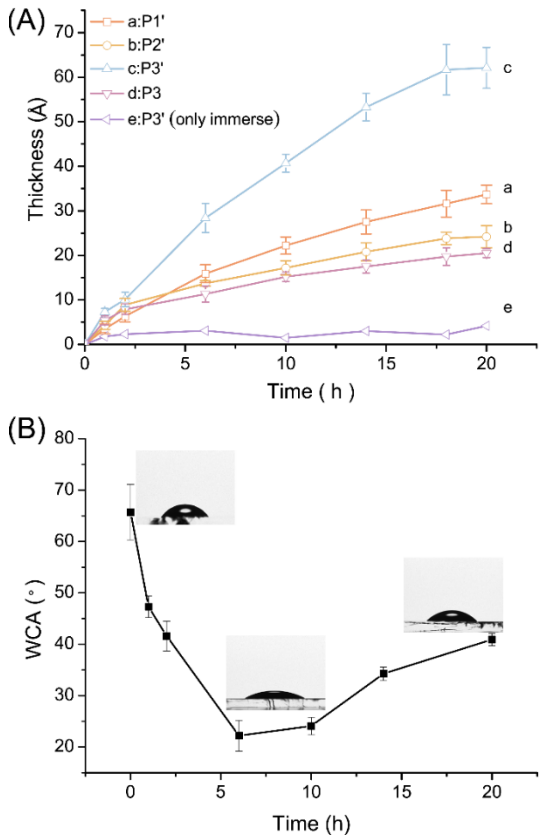

Fig. 4 (A) The adlayer thickness of PEG modified Ti substrates by e-AMs (P1'-a, P2'-b, P3'-c) and SAMs (P3-d, P3'-e), during different modification times. (B) The WCA of e-AMs of P3' on titanium substrates at different modification time.

3C) when modifying for 6 h, the WCA of surface decreased abruptly, and the wettability become very well as shown in Fig. 4B. When the density of the PEG on the surface increased further with the modification time (20 h, Fig. 3D, Fig. 4A c), the WCA of modified surface increased (Fig. 4B) compare with 6h modified surface, implying that the wettability of modified surface decreased due to the reduction of hydrogen-bonding availability between ultrahigh dense PEG chains and water as we discussed before. Thus, it is significant that the electro-assembly of P3' on Ti substrates can be used to prepare a surface with an excellent wetting ability, because the PEG density of electro-assembly P3' can reach a high value and can be modulated easily through modification time.

Anti-fouling and biocompatibility properties

To explore the anti-fouling properties of the e-AMs further, full blood serum was used. Fig. 5 shows the adsorbed serum thickness on the P3 and P3' modified substrates obtained by ellipsometry for different modification time. As shown, the adsorbed serum protein thickness of SAMs modified Ti substrates decreased as the increase of the PEG adlayers thickness. The lowest adsorbed serum average thickness was 0.38 Å, corresponding to a SAM thickness of 20.5 Å. However, the lowest adsorbed serum average thickness of P3' e-AMs modified Ti substrate was very tiny (0.22 Å) for the 6 h modified substrate, implying that the anti-fouling properties of the 6 h modified e-AMs was better than those of the 20 h modified SAMs (let alone 6 h modified SAMs) and the 20 h e-AMs modified Ti substrates. Actually, the serum adsorption value of e-AMs of different time modified substrate is consistent with the WCA value (Fig. 4B). As we know, the PEG adlayer thickness and brush density

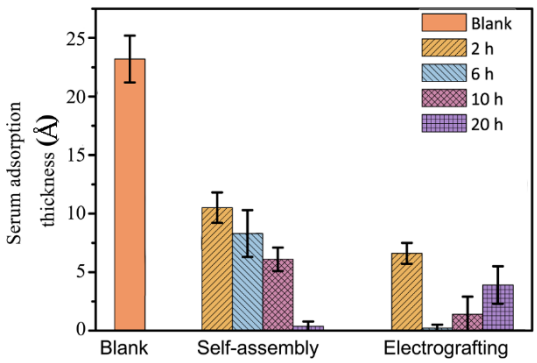

Fig. 5 Serum adsorption thickness on P3 SAMs and P3' e-AMs modified Ti substrates and blank Ti substrate ($p < 0.005$).

controlled the hydrophilicity of PEG coating, and the hydrophilicity controlled the anti-fouling properties. Obviously, the electro-assembly of P3' can be used to produce modified titanium surface with excellent anti-fouling properties in a shorter time.

As depicted in Fig. 6, the long-term anti-fouling properties were verified by LSCM image of the attachment tests of FITC-BSA on blank (A, D) Ti substrates; 20 h P3 SAMs (B, E) modified Ti substrates; 6 h P3' e-AMs modified Ti substrates (C, F). As for the fresh modified substrates, no matter for SAMs (Fig. 6B) or e-AMs (Fig. 6C), the attachment of FITC-BSA was hardly observed, meanwhile the FITC-BSA adsorption can be observed on the blank substrate (Fig. 6A). However, the adsorption for the SAMs modified sample that had been incubated in PBS buffer for 30 days (Fig. 6E) was increased and as same as that of blank Ti sample (Fig. 6D). In effect, as depicted in Fig. 6F, the adsorption for the 30 days incubated e-AMs modified samples were still hardly to be observed, implying that the e-AMs was stable and has the long-term anti-fouling property. The normalized fluorescence intensity values of FITC-BSA adsorption substrate, relative to the fluorescence intensity of Fig. 6A was showed in ESI (Fig. S13).

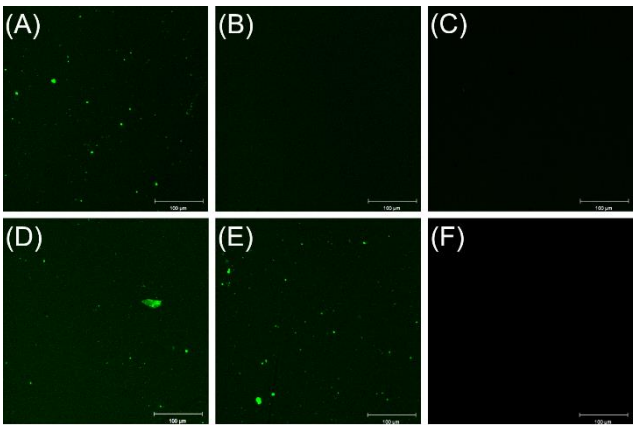

Fig. 6 The LSCM images of qualitative results of attachment tests of FITC-BSA of blank Ti substrate (A, D), SAMs of P3 20 h modified Ti substrate (B, E), and e-AMs of P3' 6 h modified Ti substrate (C, F). A, B, C-fresh, D, E, F-incubated in PBS buffer for 30 days. Scale bar is 100 μm.

As depicted in Fig. 7, the long-term anti-fouling properties and biocompatibility were also verified by the attachment tests of platelet on blank (A, D) Ti substrates; 20 h P3 SAMs (B, E) modified Ti substrates; 6 h P3' e-AMs modified Ti substrates (C, F). There were some activated platelet on the Fig. 7A. Meanwhile, only few platelet can be observed on the Fig.7 B and C. The results revealed that the

PEG coating against platelet adsorption on the titanium surfaces and the biocompatibility of the modified surfaces were better than the blank surfaces, because the platelet was not aggregated and activated on the modified surfaces (Fig.7 B and C). After 30 days, the attachment of platelet on blank (Fig. 7D) and SAMs modified substrate (Fig. 7E) was increased and the platelets were aggregated and activated, but the e-AMs modified substrate (Fig. 7F) still has no platelet aggregated and activated as same as the fresh e-AMs modified substrate (Fig. 7C). These results illustrated that the e-AMs modified substrates not only possess the platelet adsorption resistance ability and good biocompatibility, but also have the long-term anti-fouling properties.

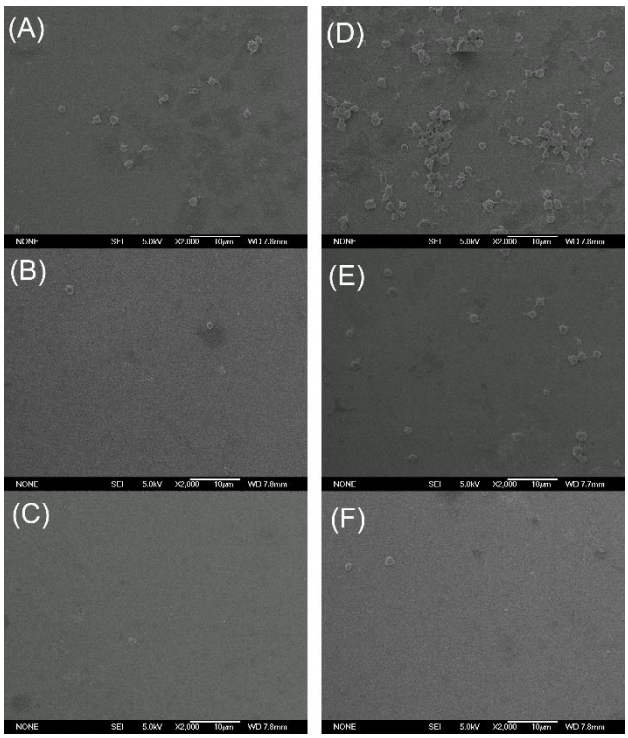

Fig. 7 SEM images of attachment tests of platelet of blank Ti substrate (A, D), SAMs of P3 20 h modified Ti substrate (B, E), and e-AMs of P3' 6 h modified Ti substrate (C, F). A, B, C-fresh, D, E, F-incubated in PBS buffer for 30 days. Scale bar is 10 μm.

The study of the stability

The stability of the adlayers is very important for practical use. Fig. 8 shows the thickness changes of the PEG adlayers formed using SAMs and e-AMs for a period of four weeks. As shown, after two weeks the remaining normalized layer thickness values of the P1, P2, and P3 SAMs (20 h) were 42.3%, 34.1%, and 65.3%, respectively, and after four weeks, the values were 32.8%, 22.1%, and 43.9%, respectively. Whereas after two weeks, the remaining normalized layer thickness values of the P1' (20 h), P2' (20 h), P3' (20 h) and P3' (6 h) e-AMs were 91.6%, 60.7%, and 94.4%, and 96.1%, respectively, after four weeks, the values were 83.5%, 46.2%, and 89.5%, and 90.9%, individually. Obviously, the e-AMs exhibited more stability than the SAMs. The decrease of thickness of PEG adlayers might attribute to the drop of PEG brush from the substrate surfaces and the oxidative degradation of PEG.[4] As reported, the PEG-catechol of SAMs was attached onto the Ti substrate through stable catechol-titanium co-ordination bonding or hydrogen bonding.[17] The parts of PEG that attached onto the Ti substrate by hydrogen bonding do not have long-term stability and easy drop from the substrate, which resulted in a significant decrease in the remaining normalized layer thickness values of SAMs. As we discussed before, the PEG of e-AMs adlayers were attached onto the Ti substrate through catechol-titanium co-ordination bonding, the PEG brush was stable and not easy to drop from the surfaces. Thus, the decrease of thickness of e-AMs could attribute to the oxidative degradation of PEG. In conclusion, the thickness of e-AMs of P1' and P3' has only decreased about 10 % after four weeks, the stability was much better than that of SAMs. As shown in the data, the stability of the e-AMs formed by P2' is not as good as that of P1' and P3'. A possible reason for this reduced stability is that the Ti substrate was covered by some P2" (Scheme 1) through hydrogen bonding; but it was still more stable than the SAMs of P2. We have also measured the change of WCA of those substrates, which was shown in the ESI (Table S2) and proved the long-term stability of e-AMs. All of above results unambiguously demonstrated that e-AMs were stable, which is important for the practical application.

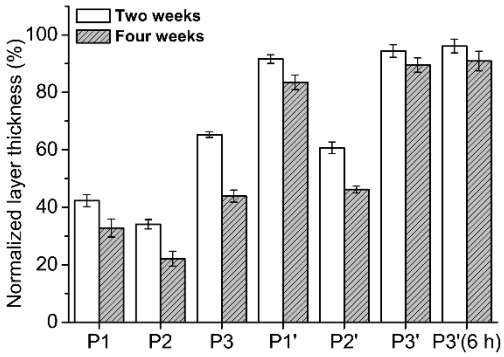

Fig. 8 Stability of the PEG adlayers on the Ti substrate. The remaining normalized layer thickness values, relative to the initial thickness (=100%) after two weeks and four weeks ($p < 0.01$).

Conclusion

Herein, we present a facile and effective approach for titanium surface antifouling modification via PEG-*o*-quinone electro-assembly technique. PEG modified titanium substrate with ultrahigh grafting density could be produced via this approach, but it could not be produced by using PEG-catechol self-assembly approach. The grafting density of adlayers produced by this approach (e-AMs) could be modulated in a wide range. By this reason, the wetting ability of PEG adlayers also could be modulated and the optimal density for the best wetting ability could be found. The optimal density means the PEG can cover the substrate fully with a suitable PEG density and good wetting ability, for the wetting ability will decrease if the PEG density is too high. Furthermore, it was verified that there is a correlation between the anti-fouling properties and the wetting ability of the modified surface, i.e. good wetting ability of PEG modified surface is necessary for the antifouling surface. We also verified that the electro-assembly of PEG-o-quinone could be used to produce PEG adlayer with long-term stability for against full blood serum, FITC marked BSA and platelet adsorption. In additional, this approach is also environmentally friendly that can operate in neutral aqueous solutions under ambient conditions and the mPEG-o-quinone solution can be

reuse for many times. These features are very important for the surface modification field of biomaterials and medically implanted devices.

Acknowledgements

The authors thank Prof. Guangzhao Zhang and Dr. Guangming Liu of the Department of Chemical Physcics of USTC for the ellipsometry analysis. This work was supported by the Ministry of Science and Technology of China (Grant No. 2012CB933802) and the National Natural Science Foundation of China (Grant No. 21374109).

Notes and references

CAS Key Laboratory of Soft Matter Chemistry, Department of Polymer Science and Engineering, University of Science and Technology of China, 230026, Hefei, People's Republic of China; E-mails: wangyanm@ustc.edu.cn

1. M. Niinomi, *Metall. Mater. Trans. A* 2002, **33**, (3), 477-486.
2. G. Müller, H. Benkhai, R. Matthes, B. Finke, W. Friedrichs, N. Geist, W. Langel and A. Kramer, *Biomaterials*, 2014, **35**, 5261-5277.
3. C.-J. Pan, Y.-H. Hou, B.-B. Zhang, Y.-X. Dong and H.-Y. Ding, *J. Mater. Chem. B*, 2014, **2**, 892-902.
4. R. Konradi, B. Pidhatika, A. Muhlebach and M. Textor, *Langmuir*, 2008, **24**, 613-616.
5. S. Zürcher, D. Wäckerlin, Y. Bethuel, B. Malisova, M. Textor, S. Tosatti and K. Gademann, *J. Am. Chem. Soc.*, 2006, **128**, 1064-1065.
6. S. Krishnan, C. J. Weinman and C. K. Ober, *J. Mater. Chem.*, 2008, **18**, 3405-3413.
7. A. S. de León, J. Rodríguez-Hernández and A. L. Cortajarena, *Biomaterials*, 2013, **34**, 1453-1460.
8. K. Cai, A. Rechtenbach, J. Hao, J. Bossert and K. D. Jandt, *Biomaterials*, 2005, **26**, 5960-5971.
9. E. Wischerhoff, N. Badi, J.-F. Lutz and A. Laschewsky, *Soft Matter*, 2010, **6**, 705-713.
10. H. Liu, Y. Li, K. Sun, J. Fan, P. Zhang, J. Meng, S. Wang and L. Jiang, *J. Am. Chem. Soc.*, 2013, **135** (20), 7603−7609.
11. F. Cao, X. Zhu, Z. Luo, J. Xing, X. Shi, Y. Wang and H. Cheradame, *Electrophoresis*, 2011, **32**, 2874-2883.
12. A. Venault, H.-S. Yang, Y.-C. Chiang, B.-S. Lee, R.-C. Ruaan and Y. Chang, *ACS Appl. Mater. Inter.*, 2014, **6**, 3201-3210.
13. J. Pei, H. Hall and N. D. Spencer, *Biomaterials*, 2011, **32**, 8968-8978.
14. J. H. Kang, E. J. Siochi, R. K. Penner and T. L. Turner, *Compos. Sci. Technol.*, 2014, **96**, 23-30.
15. T. H. Anderson, J. Yu, A. Estrada, M. U. Hammer, J. H. Waite and J. N. Israelachvili, *Adv. Funct. Mater.* , 2010, **20**, 4196-4205.
16. J. Sedó, J. Saiz-Poseu, F. Busqué and D. Ruiz-Molina, *Adv. Mater.*, 2013, **25**, 653-701.
17. Q. Ye, F. Zhou and W. Liu, *Chem. Soc. Rev.*, 2011, **40**, 4244-4258.
18. T. Gillich, E. M. Benetti, E. Rakhmatullina, R. Konradi, W. Li, A. Zhang, A. D. Schlüter and M. Textor, *J. Am. Chem. Soc.*, 2011, **133**, 10940-10950.
19. B. Malisova, S. Tosatti, M. Textor, K. Gademann and S. Zürcher, *Langmuir*, 2010, **26**, 4018-4026.
20. S. Yuan, D. Wan, B. Liang, S. O. Pehkonen, Y. P. Ting, K. G. Neoh and E. T. Kang, *Langmuir*, 2011, **27**, 2761-2774.
21. C. d. Zobrist, J. Sobocinski, J. l. Lyskawa, D. Fournier, V. r. Miri, M. Traisnel, M. Jimenez and P. Woisel, *Macromolecules*, 2011, **44**, 5883-5892.
22. T. Shalev, A. Gopin, M. Bauer, R. W. Stark and S. Rahimipour, *J. Mater. Chem.*, 2012, **22**, 2026-2032.
23. Z.-Y. Xi, Y.-Y. Xu, L.-P. Zhu, Y. Wang and B.-K. Zhu, *J. Membrane Sci.*, 2009, **327**, 244-253.
24. J. Jiang, L. Zhu, L. Zhu, H. Zhang, B. Zhu and Y. Xu, *ACS Appl. Mater. Inter.*, 2013, **5**, 12895-12904.
25. K. Kang, S. Lee, R. Kim, I. S. Choi and Y. Nam, *Angew. Chem. Int. Edit.*, 2012, **51**, 13101-13104.
26. Q. Wei, T. Becherer, P. L. M. Noeske, I. Grunwald and R. Haag, *Adv. Mater.* 2014, **26**, (17), 2688-2693.
27. X. Shi, S. Ostrovidov, Y. Shu, X. Liang, K. Nakajima, H. Wu and A. Khademhosseini, *Langmuir*, 2013, **30**, 832-838.
28. Y. Cong, T. Xia, M. Zou, Z. Li, B. Peng, D. Guo and Z. Deng, *J. Mater. Chem. B*, 2014, **2**, 3450-3461.
29. Sundaram, H. S.; Han, X.; Nowinski, A. K.; Ella-Menye, J.-R.; Wimbish, C.; Marek, P.; Senecal, K.; Jiang, S., *ACS Appl. Mater. Inter.*, 2014, 6, (9), 6664-6671.
30. H. S. Kim, H. O. Ham, Y. J. Son, P. B. Messersmith and H. S. Yoo, *J. Mater. Chem. B*, 2013, **1**, 3940-3949.
31. T. A. Annan and D. G. Tuck, *Can. J. Chem.*, 1989, **67**, 1807-1814.
32. K. Kim, H. Yang, S. Jon, E. Kim and J. Kwak, *J. Am. Chem. Soc.*, 2004, **126**, 15368-15369.
33. I. S. Choi and Y. S. Chi, *Angew. Chem. Int. Edit.*, 2006, **45**, 4894-4897.
34. K. Huang, B. P. Lee, D. R. Ingram and P. B. Messersmith, *Biomacromolecules*, 2002, **3**, 397-406.
35. B. P. Lee, J. L. Dalsin and P. B. Messersmith, *Biomacromolecules*, 2002, **3**, 1038-1047.
36. I. Munaweera, A. Aliev and K. J. Balkus, *ACS Appl. Mater. Inter.*, 2013, **6**, 244-251.
37. C. M. De Silva, B. Pandey, F. Li and T. Ito, *Langmuir*, 2013, **29**, 4568-4573.
38. HILFIKER, J. N., SYNOWICKI, R. A., BUNGAY, C. L., CARPIO and R., *Spectroscopic ellipsometry for polymer thin films*, PennWell, Tulsa, OK, ETATS-UNIS, 1998, **41**, 101−110.
39. T. Weber, M. Bechthold, T. Winkler, J. Dauselt and A. Terfort, *Colloids Surf. B Biointerfaces*, 2013, **111**, 360-366.
40. Y. Ding, Z. Yang, C. W. C. Bi, M. Yang, J. Zhang, S. L. Xu, X. Lu, N. Huang, P. Huang and Y. Leng, *J. Mater. Chem. B*, 2014, **2**, 3819-3829.
41. B.-L. He, B. Dong and H.-L. Li, *Electrochem. Commun.* , 2007, **9**, 425-430.
42. J. L. Dalsin, L. Lin, S. Tosatti, J. Vörös, M. Textor and P. B. Messersmith, *Langmuir*, 2004, **21**, 640-646.
43. R. Ogaki, O. Zoffmann Andersen, G. V. Jensen, K. Kolind, D. C. E. Kraft, J. S. Pedersen and M. Foss, *Biomacromolecules*, 2012, **13**, 3668-3677.
44. W. Yandi, S. Mieszkin, P. Martin-Tanchereau, M. E. Callow, J. A. Callow, L. Tyson, B. Liedberg and T. Ederth, *ACS Appl. Mater. Inter.* 2014, **6**, 11448-11458.

